is given on any current masthead page.

References and Notes

(1) Indian Institute of Technology, Madras.
(2) Indian Institute of Science, Bangalore.
(3) (a) M. Elkins and L. Hunter, *J. Chem. Soc.*, 1346 (1938); (b) D. N. Purohit, *Talanta*, **14**, 353 (1967), and references cited therein; (c) A. Chakravorty, B. Behera, and P. S. Zacharias, *Inorg. Chim. Acta*, **2**, 85 (1968); (d) B. Behera and A. Chakravorty, *J. Inorg. Nucl. Chem.*, **31**, 1791 (1969); *Inorg. Chim. Acta*, **4**, 372 (1970); (e) P. S. Zacharias and A. Chakravorty, *Inorg. Chem.*, **10**, 1961 (1971); (f) P. S. Zacharias, Ph.D. Thesis, Indian Institute of Technology, Kanpur, India, 1971.
(4) V. P. Chacko and P. T. Manoharan, *J. Magn. Reson.*, **22**, 7 (1976).
(5) G. C. Dwivedi and R. C. Srivastava, *Acta Crystallogr., Sect. B*, **27**, 2316 (1971).
(6) R. H. Holm and M. J. O'Connor, *Prog. Inorg. Chem.*, **14**, 241 (1971) (a review of the stereochemistry of bis(chelate) complexes), and references cited therein.
(7) (a) R. C. Hoy and R. H. Morriss, *Acta Crystallogr.*, **22**, 476, (1967); (b) J. Iball and C. H. Morgan, *J. Chem. Soc. A*, 52 (1967); (c) N. A. Bailey, P. M. Harrison, and R. Mason, *Chem. Commun.*, 559 (1968).
(8) Programs for the IBM 370/155 used for this work were all locally written except Johnson's ORTEP thermal ellipsoid plot program. Atomic scattering factors for all atoms were taken from "International Tables for X-ray Crystallography", Vol. III, J. S. Kasper and K. Lonsdale, Eds., Kynoch Press, Birmingham, England, 1959, p 202. Corrections for the real part of the anomalous scattering of nickel and chlorine were taken from D. T. Cromer, *Acta Crystallogr., Sect. A*, **18**, 17 (1965).
(9) Supplementary material.
(10) The first figure in parentheses following an average value is the mean deviation ($\{\sum(x-\bar{x})^2/[m(m-1)]\}^{1/2}$) of the average calculated over m measurements, and the second figure is the root-mean-square value of the standard deviations in individual measurements ($\{\sum\sigma(x)^2/m\}^{1/2}$).
(11) Equations of the least-squares planes are in the form $lx + my + nz = D$ where the coordinates, x, y, z, are in Å and are referred to a Cartesian coordinate system with $\vec{i}$ along the a axis and $\vec{j}$ along the b^* axis. D is the perpendicular distance of the mean plane from the origin.
(12) G. S. Hall and R. H. Soderberg, *Inorg. Chem.*, **7**, 2300 (1968).
(13) See, for example, R. Eisenberg, *Prog. Inorg. Chem.*, **12**, 338 (1970).

Contribution from the Institut für Physikalische und Theoretische Chemie, Tübingen, West Germany, and the Institut für Anorganische Chemie, Heidelberg, West Germany

Molecular Structures of Di-μ-oxy-diselenium Octafluoride, $Se_2O_2F_8$, and Di-μ-oxy-ditellurium Octafluoride, $Te_2O_2F_8$

HEINZ OBERHAMMER* and KONRAD SEPPELT

Received September 7, 1978

The molecular structures of $Se_2O_2F_8$ and $Te_2O_2F_8$ have been determined in the gas phase by electron diffraction. The skeleton of both molecules is a planar four-membered ring, with Se–O = 1.779 (7) Å, ∠SeOSe = 97.5 (0.5)°, Te–O = 1.918 (9) Å, and ∠TeOTe = 99.5 (0.6)°. All geometric parameters are r_g values, and error limits are 3 times the standard deviations. The configuration around the chalcogen atoms deviates considerably from octahedral with equatorial X–F bonds about 0.03–0.04 Å shorter than the axial X–F bonds. The geometric parameters and vibrational amplitudes are given.

Introduction

The structural behavior of the heavier main-group element oxyfluorides became of interest only a few years ago; e.g., many new selenium and tellurium oxyfluorides are stable and inert materials and thus are preferable compounds for structural investigations.[1-3] Soon it was found out that tellurium(VI) avoids double bonded oxygen,[2,3] whereas in the case of selenium at least two examples with Se–O double bonds are known: the stable SeO_2F_2 and the highly unstable $SeOF_4$.[4,5] The latter stabilizes by forming a dimer, $Se_2O_2F_8$.[5] The analogous tellurium oxide fluoride $Te_2O_2F_8$ was found soon afterward, although the monomeric species $TeOF_4$ has not yet been detected.

Vibrational spectroscopy and especially ^{19}F NMR spectroscopy quickly led to the four-membered ring structure of the two title molecules. This has been confirmed by repeated measurements.[6] An earlier investigation of the gas-phase structures of F_5SOSF_5, $F_5SeOSeF_5$, and $F_5TeOTeF_5$ showed results that raised the question of (pd)π bonding.[1] A comparison of the geometric parameters of the strained XO_2X skeleton with the respective parameters of $F_5X{-}O{-}XF_5$ molecules may give more detailed information about the question of (pd)π bonding in such highly oxidized species.

Experimental Section

$Se_2O_2F_8$. This compound was prepared by pyrolysis of $Na^+OSeF_5^-$ via the intermediate formation of $SeOF_4$.[5] It is often the decomposition product of many $OSeF_5$ species like $As(OSeF_5)_3$ and may be purified from such a decomposition.[7] The crude product is washed with a sodium hydroxide water solution to remove all hydrolyzable compounds and then dried over P_4O_{10}. It is distilled under dynamic vacuum several times to remove traces of SeF_6. The final physical data are mp −12 °C and bp 65 °C. The absence of SeF_6, $HOSeF_5$, $F_5SeOSeF_5$, and other impurities may be checked by ^{19}F NMR spectroscopy. $Se_2O_2F_8$ is a clear liquid with an unpleasant odor.

$Te_2O_2F_8$. A new method of preparation described as the original method[5] by pyrolysis of $Li^+OTeF_5^-$ turned out to be ineffective. Thus $B(OTeF_5)_3$[8] is sublimed at room temperature through a 600 °C quartz tube with a length of 60 cm. The products are frozen out at −196 °C. Trap to trap distillation in a glass vacuum line removes the major impurities $B(OTeF_5)_3$, TeF_6, and BF_3. (Alkaline water leads to complete hydrolysis!) The product is then dried over P_4O_{10} and again distilled under dynamic vacuum. The yield exceeds 80%.

$$B(OTeF_5)_3 \xrightarrow{600\ °C} BF_3 + {}^3/_2Te_2O_2F_8$$

$Te_2O_2F_8$ is a colorless liquid with a garlic-like smell: mp 28 °C; bp 77.5 °C.

The diffraction intensities were recorded with a Balzers Diffractograph, Model KD-G2, at two camera distances, 50 and 25 cm.[9] Kodak Electron Image plates (18 × 13 cm) were used. Details of the experiment are summarized in Table I. The electron wavelength was determined from ZnO diffraction patterns. Four plates were exposed for each camera distance, two of which were selected for the structure determination. The procedures for data analysis and background refinement are described in ref 10. The averaged modified molecular intensities for the two camera distances are shown in Figures 1 and 2. (Numerical values of the total intensities are available as supplementary material.)

Structure Analysis

Primary molecular models with D_{2h} symmetry, obtained from analysis of the radial distribution functions (Figures 3 and 4), were refined by least-squares procedures based on the molecular intensities. A diagonal weight matrix was used with

---

*To whom correspondence should be addressed at the Institut für Physikalische und Theoretische Chemie.

0020-1669/79/1318-2226$01.00/0

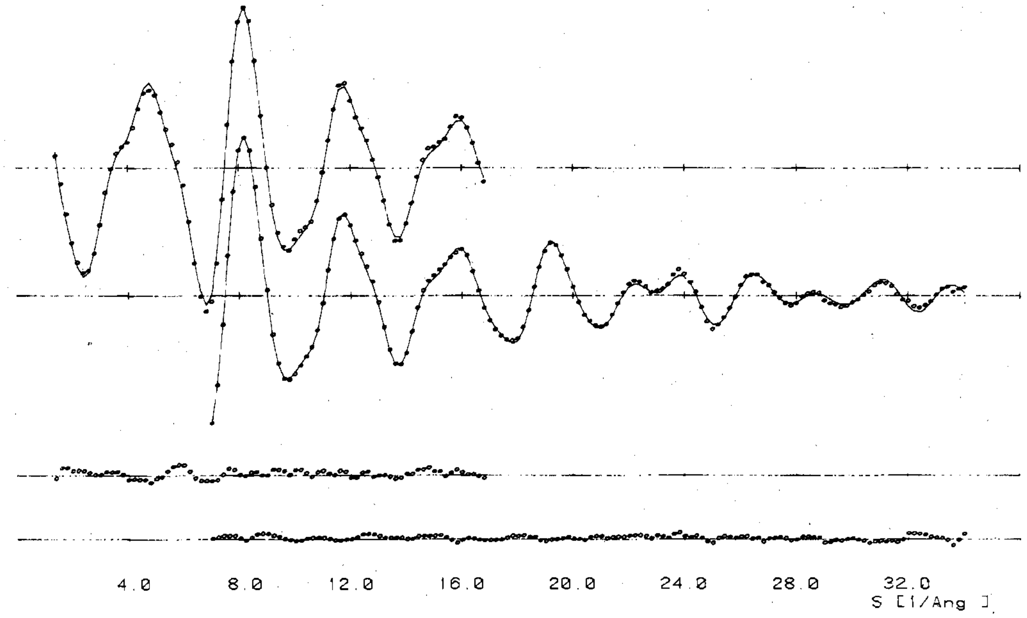

Figure 1. Experimental (○) and calculated (—) modified molecular intensities and differences for $Se_2O_2F_8$.

Table I. Experimental Details

	$Se_2O_2F_8$		$Te_2O_2F_8$	
nozzle-plate dist, cm	50	25	50	25
sample temp, °C	−24	−25	−6	−6
nozzle temp, °C	10	10	15	15
camera pressure, torr	5×10^{-6}	8×10^{-6}	5×10^{-6}	5×10^{-6}
exposure time, s	20–40	40–90	10–30	25–60
nozzle diameter, mm	0.3	0.3	0.3	0.3
electron wavelength, Å	0.049 31 (1)	0.049 24 (1)	0.049 27 (1)	0.049 35 (1)
s range, $Å^{-1}$	1.4–16.8	7–34	1.4–16.8	8–35

Table II. Results of Least-Squares Analysis[a]

	$Se_2O_2F_8$		$Te_2O_2F_8$	
(a) Geometric Parameters (r_g Values) and Mean-Square Amplitudes for Bonded Distances				
X–O, Å	1.779 (7)		1.918 (9)	
$X–F_{eq}$, Å	1.668 (12)		1.802 (11)	
$X–F_{ax}$, Å	1.698 (10)		1.848 (11)	
∡XOX, deg	97.5 (0.5)		99.5 (0.6)	
∡OXO, deg	82.5 (0.5)		80.5 (0.6)	
$∡F_{eq}XF_{eq}$, deg	92.4 (0.5)		92.1 (1.2)	
$∡F_{ax}XF_{ax}$, deg	175.6 (0.8)		174.3 (0.8)	
l(X–O) = l(X–F), Å	0.046 (7)		0.053 (8)	
(b) Nonbonded Interatomic Distances and Mean-Square Amplitudes in Å				
$F_1\cdots F_3$	2.35 (1)	0.073 (8)	2.54 (1)	0.072 (7)
$F_3\cdots F_4$	2.42 (3)		2.60 (3)	
$O\cdots F_1$	2.49 (1)		2.71 (1)	
$O\cdots F_3$	2.49 (2)		2.72 (2)	
$F_1\cdots F_2$	3.38 (2)	0.060 (15)	3.69 (2)	0.067 (14)
$O\cdots F_4$	3.45 (1)		3.72 (1)	
$O\cdots O'$	2.34 (2)	0.055[b]	2.48 (2)	0.055[b]
$X\cdots X'$	2.67 (2)	0.039 (5)	2.93 (2)	0.038 (3)
$X\cdots F_1'$	3.22 (2)	0.083 (10)	3.54 (2)	0.092 (13)
$X\cdots F_3'$	4.01 (2)	0.075 (10)	4.38 (2)	0.090 (15)
$F_1\cdots F_1'$	2.81 (3)	0.150[b]	3.11 (3)	0.165 (90)
$F_1\cdots F_2'$	4.40 (3)	0.109 (15)	4.82 (3)	0.136 (20)
$F_1\cdots F_3'$	4.42 (2)		4.83 (2)	
$F_3\cdots F_3'$	4.98 (4)	0.119 (55)	5.44 (4)	0.159 (84)
$F_3\cdots F_4'$	5.38 (3)		6.03 (3)	
(c) Agreement Factors (%)				
R_{50}	5.7		4.0	
R_{25}	5.3		10.4	

[a] See Figure 5 for the atom numbering scheme. [b] Assumed.

Table III. Correlation Coefficients Larger Than 0.6

	$Se_2O_2F_8$	$Te_2O_2F_8$
r(X–O)/∡XOX	−0.95	−0.98
r(X–O)/l(X–F)	−0.71	
$r(X–F_{eq})/r(X–F_{ax})$	−0.96	−0.84
$r(X–F_{eq})/l(X–F)$	0.85	0.70
$r(X–F_{ax})/∡F_{ax}XF_{ax}$	0.62	
$r(X–F_{ax})/l(X–F)$	−0.76	
∡XOX/l(X–F)	0.67	

elements increasing exponentially from 0.25 to 1 for $s < 4$ $Å^{-1}$ and $s < 9$ $Å^{-1}$ for the 50- and 25-cm data, respectively, and decreasing exponentially from 1 to 0.1 for $s > 15$ $Å^{-1}$ and $s > 30$ $Å^{-1}$. All other elements were chosen to be 1. The experimental molecular intensities were interpolated in steps of $\Delta s = 0.2$ $Å^{-1}$.

Two possible deviations from D_{2h} symmetry of the molecules were considered in the least-squares analysis: (1) nonplanarity of the X_2O_2 rings (C_{2v} symmetry) and (2) torsion of the XF_4 groups around X···X axis in opposite directions (D_2 symmetry). In all cases, however, the least-squares procedures converged toward D_{2h} symmetry with deviations smaller than the respective σ values. With the constraint of D_{2h} symmetry in the final least-squares analyses and with assumptions for the vibrational amplitudes which are indicated in Table II, six geometric parameters and nine mean-square amplitudes were refined simultaneously. Although some correlation coefficients (Table III) are large, the least-squares procedures converged after eight cycles to the results given in Table II, independent of the starting geometry. (The full correlation matrices are available as supplementary material.) Starting values for bond lengths and bond angles were varied by 0.05 Å and 5°, respectively.

Introducing separate vibrational amplitudes for the X–F and X–O bonds caused problems with convergence of the least-squares procedure. The assumption of equal mean-square

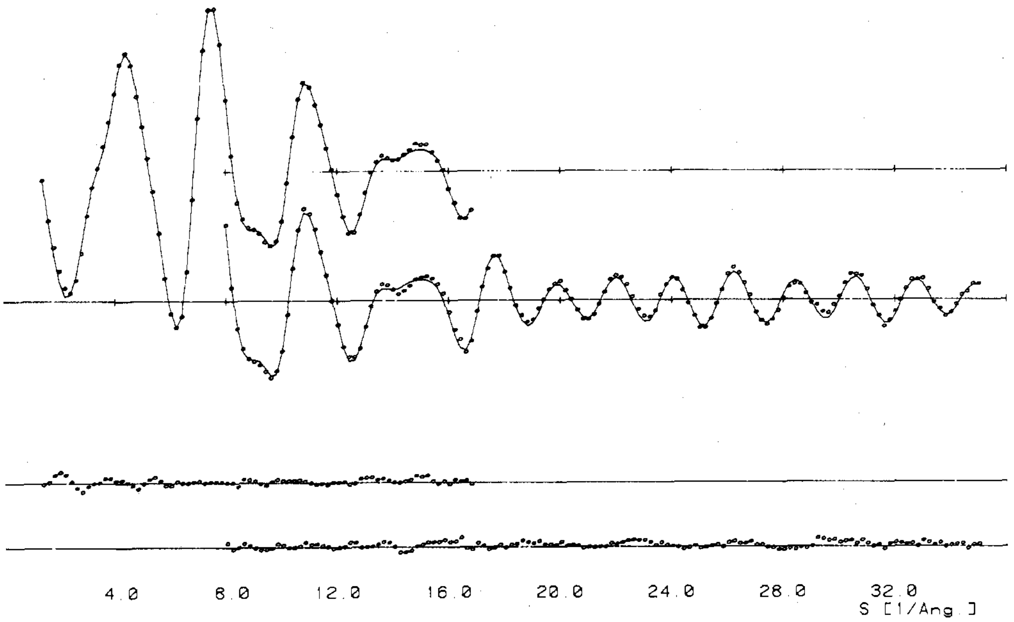

Figure 2. Experimental (○) and calculated (—) modified molecular intensities and differences for $Te_2O_2F_8$.

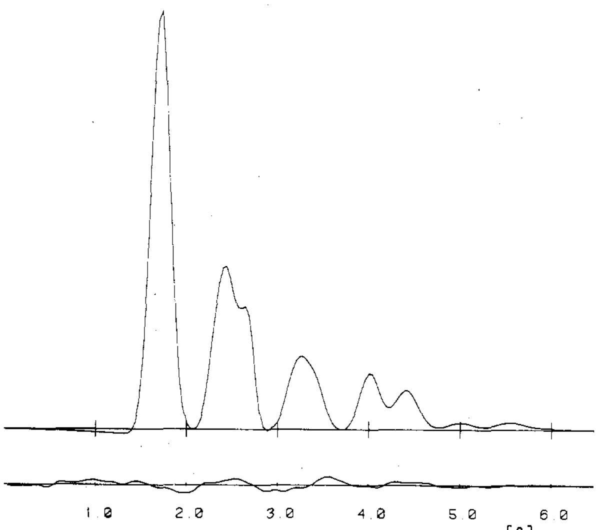

Figure 3. Experimental radial distribution function and difference curve for $Se_2O_2F_8$.

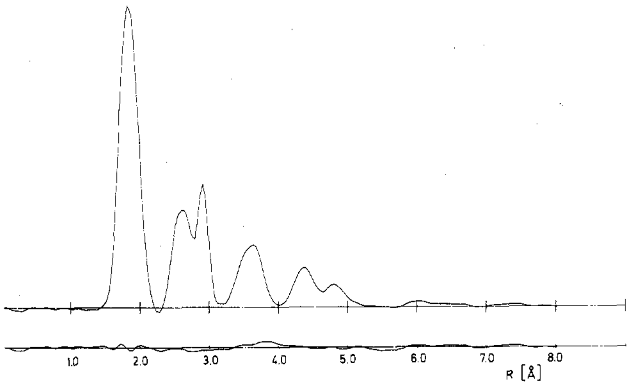

Figure 4. Experimental radial distribution function and difference curve for $Te_2O_2F_8$.

amplitudes for all bonded distances, however, introduces errors in the bond lengths which are smaller than the error limits of Table II, according to our estimates. This was indicated by several tests assuming differences of 0.005 Å between the various amplitudes.

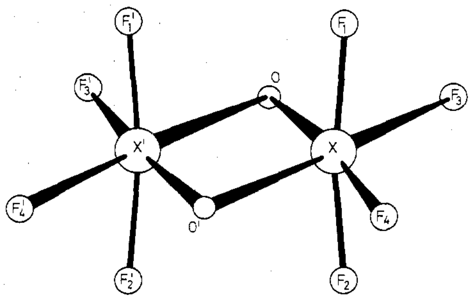

Figure 5. Molecular model for $X_2O_2F_8$.

Table IV. Geometry of the Molecular Skeletons of $X_2O_2F_8$ and X_2OF_{10} and Schomaker-Stevenson Bond Lengths (r_{SS})

		X = Se	X = Te
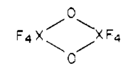	X–O	1.779 (7)	1.918 (9)
	∡XOX	97.5 (0.5)	99.5 (0.6)
	X···X	2.67 (2)	2.93 (2)
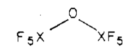	X–O	1.697 (13)	1.832 (12)
	∡XOX	142.4 (1.9)	145.5 (2.1)
	X···X	3.21 (3)	3.50 (3)
	r_{SS}(X–O)	1.82	2.00
	r_{SS}(X=O)	1.60	1.78
	r_{SS}(X–X)	2.34	2.74

The final results of the least-squares analyses are summarized in Table II. Error limits are 3 times the standard deviations.

Discussion

The proposed four-membered ring structure of $Se_2O_2F_8$ and $Te_2O_2F_8$ (Figure 5) has been confirmed. It appears now that such a ring formation between two heavy nonmetal atoms and two bridging oxygens is a general building principle. The driving force of such ring formation must be the tendency to avoid oxygen double bonds. Other examples are $TeO_8(OH)_2^{6-}$, $I_2O_8(OH_2)^{4-}$, and $As_2O_4F_8^{2-}$.[11-13] The most recent example of such four-membered ring formation was found by the X-ray structure analysis of IO_2F_3, which turned out to be an oxygen-bridged dimer, $I_2O_4F_6$.[14]

Table IV summarizes the geometric parameters for the chalcogen–oxygen skeletons of the doubly bridged oxide fluorides $Se_2O_2F_8$ and $Te_2O_2F_8$ and the bis(pentafluorochalcogen) oxides $F_5X–O–XF_5$.

In contrast to F_5SOSF_5 etc. the bond angles at the chalcogen atoms of the title compounds deviate considerably from the octahedral configuration, these deviations being slightly stronger in the tellurium compound. The equatorial X–F bonds are about 0.03-0.04 Å shorter than the axial bonds.

The comparison of the chalcogen–oxygen skeletons shows that the bond angle at oxygen in the ring compounds has to be about 45° smaller than in the sterically strained open-chain compounds F_5XOXF_5.[1] An additional effect is a considerable lengthening of the X–O bonds upon ring formation of about 0.08–0.09 Å. Two effects may account for this increase in the X–O bond lengths.

(1) Steric repulsion between the chalcogen atoms in the four membered rings causes lengthening of the X–O bonds. The X···X distances (2.67 ± 0.02 and 2.93 ± 0.02 Å, respectively) are much shorter than the respective van der Waals distances (4.00 and 4.40 Å). In the selenium compound the Se···Se distance is only 0.33 Å longer than the Schomaker–Stevenson value for a Se–Se single bond. This difference is even smaller for the tellurium compound (0.19 Å). If the interaction between the chalcogen atoms at such close contact were repulsive, we would expect X–O bond lengths considerably longer than the Schomaker–Stevenson values. The result of the structure determination, i.e., X–O bonds shorter than expected for single bonds, indicates that the interaction between the chalcogen atoms is bonding rather than repulsive. Such bonding could result from overlap between d_{xz} orbitals (if the ring is in the xy plane with the X atoms on the x axis), provided that these orbitals are populated, maybe by some back-donation. A similar situation has been observed for tetrafluoro-1,3-diselenetane $(F_2CSe)_2$, where the short Se–C bond in this strained four-membered ring can be explained by bonding interaction between the diagonal selenium atoms.[15]

(2) A strong decrease in the oxygen bond angle reduces the possibility for $(pd)\pi$ bonding between the oxygen lone pairs and chalcogen d orbitals, since the p character of the lone pairs decreases with decreasing bond angle. In addition to this the increased p character of the oxygen bonding orbitals results in lengthening of the X–O bonds. As a matter of fact the X–O bonds do lengthen considerably upon ring formation, but they are still shorter than the respective Schomaker–Stevenson values by about 0.04–0.05 Å. A similar correlation between oxygen bond angle and bond length was observed for methylcyclosiloxanes.[16] In the tetramer and larger rings (up to hexamer) the oxygen bond angle is close to the value for the nonstrained siloxane (about 145°), and the Si–O bond lengths are short (1.620 ± 0.003 Å). For the trimer, however, the SiOSi angle is constrained to be smaller (131°), and the Si–O bond length is increased to 1.635 ± 0.002 Å.

Tossel and Gibbs have demonstrated that the large bridging angle in siloxanes is reproduced correctly by CNDO/2 calculations by omitting the silicon 3d orbitals in the basis set.[17] Nevertheless, the $(pd)\pi$ concept might still hold for the presented molecules, as the electron withdrawal by the fluorine atoms and the high formal and effective nuclear charge on the central atoms will favor the $(pd)\pi$ concept.

Registry No. $Se_2O_2F_8$, 51590-98-8; $Te_2O_2F_8$, 51590-99-9; $B(OTeF_5)_3$, 40934-88-1.

Supplementary Material Available: Experimental scattering intensities $I_{tot}(s) = s^3[\varphi(s)]/\{[\varphi_{exptl}(s)][I_{at}(s) + I_{mol}(s) + I_b(s)]\}$ [$\varphi(s)$ and $\varphi_{exptl}(s)$ are the actual and experimentally determined sector functions, respectively, and $I_{at}(s)$, $I_{mol}(s)$, and $I_b(s)$ are the atomic, molecular, and extraneous background scattering] and correlation matrices (4 pages). Ordering information is given on any current masthead page.

References and Notes

(1) H. Oberhammer and K. Seppelt, *Angew. Chem., Int. Ed. Engl.*, **17**, 69 (1978); *Inorg. Chem.*, **17**, 1435 (1978).
(2) D. Lentz, H. Pritzkow, and K. Seppelt, *Inorg. Chem.*, **17**, 1926 (1978).
(3) H. Pritzkow and K. Seppelt, *Inorg. Chem.*, **16**, 2685 (1977).
(4) A. Engelbrecht and B. Stoll, *Z. Anorg. Allg. Chem.*, **292**, 20 (1957).
(5) K. Seppelt, *Angew. Chem., Int. Ed. Engl.*, **13**, 91, 92 (1974); *Z. Anorg. Allg. Chem.*, **406**, 287 (1974).
(6) J. Beattie, R. Crocombe, A. German, P. Jones, C. Marsden, G. Van Schalkwyk, and A. Bukovszky, *J. Chem. Soc., Dalton Trans.*, 1380 (1976).
(7) K. Seppelt, *Chem. Ber.*, **110**, 1470 (1977).
(8) F. Sladky, H. Kropshofer, and O. Leitzke, *J. Chem. Soc., Chem. Commun.*, 134 (1973).
(9) W. Zeil, J. Haase, and L. Wegmann, *Z. Instrumentenkd.*, **74**, 84 (1966); H. Oberhammer in "Molecular Structures by Diffraction Methods", Vol. 4, The Chemical Society, London, 1976.
(10) H. Oberhammer and J. Strähle, *Z. Naturforsch., A*, **30**, 296 (1975).
(11) O. Lindquist, *Acta Chem. Scand.*, **23**, 3062 (1969).
(12) H. Siebert and H. Wegener, *Angew. Chem., Int. Ed. Engl.*, **4**, 523 (1965).
(13) W. Haase, *Chem. Ber.*, **106**, 734 (1973); **107**, 1009 (1974).
(14) L. E. Smart, *J. Chem. Soc., Chem. Commun.*, 519 (1977).
(15) T. Wehrung, H. Oberhammer, A. Haas, B. Koch, and N. Welcman, *J. Mol. Struct.*, **35**, 253 (1976).
(16) H. Oberhammer, W. Zeil and G. Fogarasi, *J. Mol. Struct.*, **18**, 309 (1973).
(17) J. A. Tossel and G. V. Gibbs, *Acta Crystallogr., Sect. A*, **34**, 463 (1978).